



## Low cycle fatigue and creep-fatigue behavior of Ni-based alloy 230 at 850 °C

Xiang Chen<sup>a,b,\*</sup>, Zhiqing Yang<sup>b,c</sup>, Mikhail A. Sokolov<sup>b</sup>, Donald L. Erdman III<sup>b</sup>,  
Kun Mo<sup>a</sup>, James F. Stubbins<sup>a</sup>

<sup>a</sup> Department of Nuclear, Plasma, and Radiological Engineering, University of Illinois at Urbana-Champaign, 104 South Wright Street, Urbana, IL 61801, USA

<sup>b</sup> Oak Ridge National Laboratory, 1 Bethel Valley Road, Oak Ridge, TN 37831, USA

<sup>c</sup> Shenyang National Laboratory for Materials Science, Institute of Metal Research, Chinese Academy of Sciences, Shenyang 110016, China

### ARTICLE INFO

#### Article history:

Received 30 August 2012

Received in revised form

27 September 2012

Accepted 19 November 2012

Available online 27 November 2012

#### Keywords:

Creep-fatigue

Nickel based superalloys

EBSD

High-temperature deformation

Precipitation

Failure

### ABSTRACT

Strain-controlled low cycle fatigue (LCF) and creep-fatigue testing of Ni-based alloy 230 were carried out at 850 °C. The material creep-fatigue life decreased compared with its low cycle fatigue life at the same total strain range. Longer hold time at peak tensile strain further reduced the material creep-fatigue life. Based on the electron backscatter diffraction, a novel material deformation characterization method was applied, which revealed that in low cycle fatigue testing as the total strain range increased, the deformation was segregated to grain boundaries since the test temperature was higher than the material equicohesive temperature and grain boundaries became weaker regions compared with grains. Creep-fatigue tests enhanced the localized deformation, resulting in material interior intergranular cracking, and accelerated material damage. Precipitation in alloy 230 helped slip dispersion, favorable for fatigue property, but grain boundary cellular precipitates formed after material exposure to the elevated temperature had a deleterious effect on the material low cycle fatigue and creep-fatigue property.

Published by Elsevier B.V.

### 1. Introduction

The Very High Temperature Reactor (VHTR) is one of the Gen-IV reactor design concepts which embody a common goal of providing safe, longer lasting, proliferation-resistant, and economically viable nuclear energy [1]. One of the biggest challenges in the research and development of Gen-IV reactor systems is the performance and reliability issues involving structural materials for both in-core and out-of-core applications. For instance, to maintain its economic advantage over early generation reactor systems, the VHTR has a goal of using helium at temperatures higher than 900 °C and pressures up to 7 MPa for a design life of 60 years [1,2]. The operation conditions of the VHTR impose tremendous challenges to materials used in this reactor system. To be suitable for the VHTR applications, Murty et al. [3] identified that structural materials should possess the following characteristics: (1) dimensional stability against creep damage due to elevated temperatures and irradiation; (2) satisfactory mechanical properties at elevated temperatures; (3) favorable resistance to neutron radiation damage and helium embrittlement; and (4) compatibility between the structural materials and the coolant.

Currently, one of the metallic candidate materials for the intermediate heat exchanger in the VHTR is Ni-based alloy 230

(Haynes 230) because of its desirable mechanical properties at elevated temperatures. During the operation of the VHTR, the major damage mechanism for materials used as the intermediate heat exchanger is predicted to be creep-fatigue, which arises due to interaction of creep (load at elevated temperatures) and fatigue damage (temperature gradient induced thermal strain during startup and shutdown or power transients of the VHTR). In particular, the fatigue life of the material is significantly reduced when hold time at peak tensile strain is introduced. The current database regarding the mechanical properties of alloy 230, especially creep-fatigue data, is incomplete. The mechanism of the synergic interaction between creep and fatigue is not well understood.

To better understand and address these issues, low cycle fatigue (LCF) and creep-fatigue tests of alloy 230 were conducted in this study. In addition, various microanalysis techniques, including scanning electron microscopy (SEM), energy-dispersive X-ray spectroscopy (EDS), and electron backscatter diffraction (EBSD), were used to identify the underlying damage mechanism of alloy 230 under LCF and creep-fatigue tests.

### 2. Experimental

#### 2.1. Material

Alloy 230 is a solid-solution strengthening nickel–chromium–tungsten–molybdenum alloy developed by Haynes International Corporation [4]. Table 1 shows the chemical composition of

\* Corresponding author at: Oak Ridge National Laboratory, 1 Bethel Valley Road, P.O. Box 2008, Building 4500S MS-6151, Oak Ridge, TN 37831-6151, USA.  
Tel.: +1 865 574 5058; fax: +1 865 574 6095.

E-mail addresses: [chenx@ornl.gov](mailto:chenx@ornl.gov), [x.chen1009@gmail.com](mailto:x.chen1009@gmail.com) (X. Chen).

**Table 1**  
Chemical composition of alloy 230.

Elements	Concentration (wt%)
C	0.1
S	< 0.002
Cr	22.35
Ni	Balance
Mn	0.51
Si	0.3
Mo	1.21
Ti	< 0.01
Cu	0.03
Fe	0.64
Al	0.32
Co	0.07
B	0.003
P	0.005
W	14.39
La	0.022

**Table 2**  
Test matrix for LCF and creep-fatigue testing of alloy 230.

TOTAL strain range	Strain hold time
0.5%	0, 3 min in PTS <sup>a</sup>
1.0%	0, 3, 10, 30 min in PTS
1.5%	0, 3 min in PTS

<sup>a</sup> PTS, Peak tensile strain.

alloy 230. The nickel content together with chromium in alloy 230 imparts great resistance to high temperature corrosion in various environments. Tungsten and molybdenum combined with carbon in alloy 230 are largely responsible for the strength of the material. In addition, optimized ductility and creep resistance in alloy 230 are achieved by controlling the boron content in the alloy [5,6]. In this study, all the specimens were made from the as-received material in the solution-treatment condition.

## 2.2. Mechanical testing

Cylindrical specimens and a servohydraulic test frame were used for testing. The long axis of the specimen was parallel to the rolling direction of the raw material. The detailed descriptions about the specimen design, the test frame setup, and the test matrix can be found in Refs. [7,8]. Table 2 summarizes the test conditions. For LCF tests, triangular test waveforms with a strain rate of  $2.5 \times 10^{-4}$ /s were applied, whereas in creep-fatigue tests, additional hold time between 3 and 30 min on peak tensile strain were incorporated into the fatigue testing (Fig. 1). All the tests were conducted in air at 850 °C. The heating rate was 10 °C per min and after reaching the target temperature specimens were soaked in that temperature for 45 min before the start of the test to stabilize the temperature. The end-of-test criterion was the attainment of 40% decrease in the cyclic maximum tensile stress.

## 2.3. Microstructure characterization

Microstructures of the as-received material, the aged material (aging condition: 850 °C for 45 min), and post-test specimens were studied. The thermal aging mimicked the high temperature baking period during which specimens were subject to before the start of a test. The reason to investigate the aged material was to study possible microstructural changes during the thermal aging period.

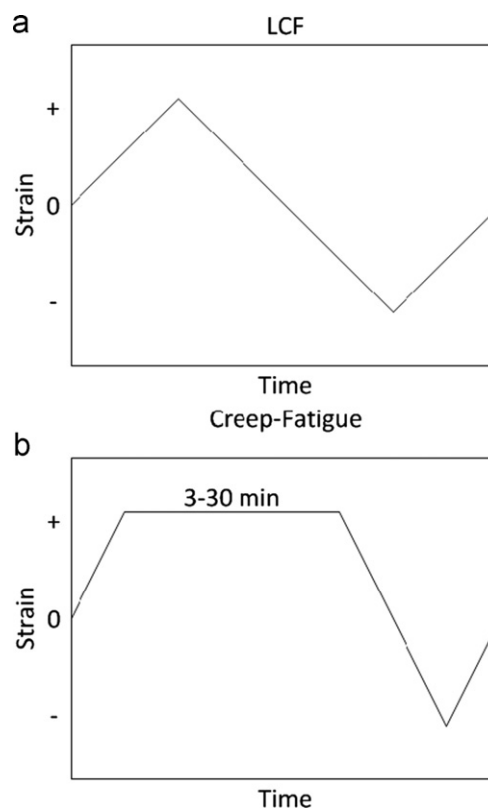


Fig. 1. LCF and creep-fatigue test waveform in (a) and (b), respectively.

Materials in different states (as-received, aged, and post-test) were cut into small strip samples first. The strip samples were polished up to 0.05  $\mu\text{m}$  with alumina suspensions. To remove the polishing damage and reveal the grain structure, polished specimens were etched with a solution consisting of 10 ml nitric acid, 10 ml acetic acid, and 15 ml hydrochloric acid between 1 and 2 min. Afterwards, JEOL 6500F, a field emission microscope with Si drift X-ray detector and high speed EBSD detector, was used for SEM, EDS, and EBSD examinations on the etched specimens. For all the micro-analysis figures of post-test specimens, the loading direction was parallel to the vertical direction of the reading plane.

Orientation imaging microscopy data collection and analysis software from TSL were used for collecting and analyzing the EBSD data. All EBSD data were collected with the specimen stage tilted at 70° to the electron beam direction and the electron acceleration voltage used was 20 kV. The specimen working distance was close to 20 mm and the image binning setting in the EBSD collection software was 4 × 4. The overall EBSD scan rate was approximately 15 FPS. EBSD analyses were done at two size scales: (1) EBSD studies on microstructure features which might influence the LCF and creep-fatigue property of alloy 230 were carried out on a relatively large scale (730  $\mu\text{m}$  × 730  $\mu\text{m}$  with a step size of 1.2  $\mu\text{m}$ ) to yield statistically significant results; and (2) EBSD scans were done on relatively small area so that microstructure features derived from SEM could be correlated with EBSD-based results.

## 3. Results and discussion

### 3.1. LCF and creep-fatigue testing

Fig. 2a shows the cyclic fatigue life of alloy 230 at different total strain ranges with various durations of the hold time at peak

Download English Version:

<https://daneshyari.com/en/article/1576440>

Download Persian Version:

<https://daneshyari.com/article/1576440>

[Daneshyari.com](https://daneshyari.com)